Two- and three-dimensional bearing capacity of footings in sand — **Source link** ↗

Andrei V. Lyamin, Rodrigo Salgado, Scott W. Sloan, Monica Prezzi

Related papers:

- Some recent research on the bearing capacity of foundations

- Two- and three-dimensional bearing capacity of foundations in clay

- Numerical limit analysis solutions for the bearing capacity factor Nγ

- Analysis of Ultimate Loads of Shallow Foundations

- Theoretical Soil Mechanics

Two- and three-dimensional bearing capacity of footings in sand

A. V. LYAMIN*, R. SALGADO†, S. W. SLOAN* and M. PREZZI†

Bearing capacity calculations are an important part of the design of foundations. Many of the terms in the bearing capacity equation, as it is used today in practice, are empirical. Shape factors could not be derived in the past because three-dimensional bearing capacity computations could not be performed with any degree of accuracy. Likewise, depth factors could not be determined because rigorous analyses of foundations embedded in the ground were not possible. In this paper, the bearing capacity of strip, square, circular and rectangular foundations in sand are determined for frictional soils following an associated flow rule using finite-element limit analysis. The results of the analyses are used to propose values of the shape and depth factors for calculation of the bearing capacity of foundations in sands using the traditional bearing capacity equation. The traditional bearing capacity equation is based on the assumption that effects of shape and depth can be considered separately for soil self-weight and surcharge (embedment) terms. This assumption is not realistic, so a different form of the bearing capacity equation is also proposed that does not rely on it.

KEYWORDS: bearing capacity; footings/foundations; limit analysis; sand

Les calculs de force portante sont un élément important de l'étude des fondations. Un grand nombre des termes utilisés dans l'équation de force portante, tels qu'ils sont utilisés à l'heure actuelle, sont empiriques. Autrefois, il n'était pas possible de dériver des coefficients de forme car on ne pouvait effectuer des calculs tridimensionnels de force portante avec la précision nécessaire. De même, il n'était pas possible de déterminer des facteurs de profondeur, car l'exécution d'analyses rigoureuses de fondations encastrées dans le sol n'était pas possible. Dans la présente communication, on détermine la force portante de fondations linéaires, carrées, circulaires et rectangulaires dans le sable pour des sols à frottement, à la suite d'une règle d'écoulement, au moyen d'une analyse des limites aux éléments finis. On utilise les résultats de ces analyses pour proposer des valeurs de coefficients de forme et de profondeur pour le calcul de la force portante des fondations dans le sable, en utilisant l'équation de force portante traditionnelle. L'équation de force portante traditionnelle est fondée sur une hypothèse d'après laquelle les effets de la forme et de la profondeur peuvent être examinés séparément pour la charge propre et la surcharge (enfouissement). Cette hypothèse n'étant pas réaliste, nous proposons également une forme d'équation de force portante diverse non basée sur cette hypothèse.

INTRODUCTION

The bearing capacity equation (Terzaghi, 1943; Meyerhof, 1951, 1963; Brinch Hansen, 1970) is one tool that geotechnical engineers employ routinely. It is used to estimate the limit unit load q_{bL} (referred to also as the limit unit bearing capacity or limit unit base resistance) that will cause a footing to undergo classical bearing capacity failure. For a footing with a level base embedded in a level sand deposit acted upon by a vertical load, the bearing capacity equation has the form

$$q_{bL} = (s_q d_q) q_0 N_q + 0.5 (s_\gamma d_\gamma) \gamma B N_\gamma \tag{1}$$

where N_q and N_γ are bearing capacity factors; s_q and s_γ are shape factors; d_q and d_γ are depth factors; q_0 is the surcharge at the footing base level; and γ is the soil unit weight below the footing base level. The limit unit load is a load divided by the plan area of the footing, and has units of stress. In the case of a uniform soil profile, with the unit weight above the level of the footing base also equal to γ, we have $q_0 = \gamma D$. The unit weight γ, the footing width B and the surcharge q_0 can be considered as given. The other terms of equation (1) must be calculated or estimated by some means.

Most theoretical work done in connection with the bearing capacity problem has been for soils following an associated flow rule. This also applies to the present paper. Until recently, the only term of equation (1) that was known rigorously was N_q (for zero self-weight), which follows directly from consideration of the bearing capacity of a strip footing on the surface of a weightless, frictional soil (Reissner, 1924; see also Bolton, 1979),

$$q_{bL} = q_0 N_q \tag{2}$$

where N_q is calculated from

$$N_q = \frac{1 + \sin\phi}{1 - \sin\phi} e^{\pi \tan\phi} \tag{3}$$

Considering a strip footing on the surface of frictional soil with non-zero unit weight γ and $q_0 = 0$, the unit bearing capacity is calculated from

$$q_{bL} = 0.5 \gamma B N_\gamma \tag{4}$$

There are two equations for the N_γ in equation (4) that have been widely referenced in the literature,

$$N_\gamma = 1.5 (N_q - 1) \tan\phi \tag{5}$$

by Brinch Hansen (1970) and

$$N_\gamma = 2 (N_q + 1) \tan\phi \tag{6}$$

by Caquot & Kerisel (1953).

Although equation (5) was developed at a time when computations were subject to greater uncertainties, it is close to producing exact values for a frictional soil following an associated flow rule for relatively low friction angle values. It tracks well the results of slip-line analyses done by

Hansen & Christensen (1969), Booker (1969) and Davis & Booker (1971) for a strip footing on the surface of a frictional soil with self-weight up to a ϕ value of roughly 40°. Martin (2005) found values of N_γ based on the slip-line method that are very accurate. Salgado (2008) proposed a simple equation, in a form similar to equation (5), that fits those values quite well:

$$N_\gamma = (N_q - 1)\tan(1{\cdot}32\phi) \tag{7}$$

Equation (1) results from the superposition of the bearing capacity due to the surcharge q_0 with that due to the self-weight of the frictional soil. While the values of N_q and N_γ satisfy a standard of rigour when used independently for the two problems for which they were developed, it is not theoretically correct to superpose the surcharge and self-weight effects (in fact, the surcharge is due to the self-weight of the soil located above the footing base). Still, while not theoretically correct, the superposition of the two solutions as in equation (1) has been used in practice for decades. Smith (2005) has recently shown that the error introduced by superposition may be as high as 25%.

In addition to superposing the effects of surcharge and self-weight, each of the two terms on the right side of equation (1) contains shape and depth factors. The shape factors are used to model the problem of the bearing capacity of a footing with finite dimensions in both horizontal directions, and the depth factors are used to model the problem in which the surcharge is in reality a soil overburden due to embedment of the footing in the soil. The equations for these factors have been determined empirically, based on relatively crude models (Meyerhof, 1963; Brinch Hansen, 1970; Vesic, 1973). Tables 1 and 2 contain the expressions more commonly used for the shape and depth factors, due to Meyerhof (1963), Brinch Hansen (1970), De Beer (1970) and Vesic (1973). The experimental data on which these equations are based are mostly due to Meyerhof

(1951, 1953, 1963), who tested both prototype and model foundations. There was some additional experimental research following the work of Meyerhof. De Beer (1970) tested very small footings bearing on sand, determining limit bearing capacity from load–settlement curves using the limit load criterion of Brinch Hansen (1963).

In this paper, we present results of rigorous analyses that we employ to obtain values of shape and depth factors for use in bearing capacity computations in sand. The shape and depth factors are determined by computing the bearing capacities of footings of various geometries placed at various depths and comparing those with the bearing capacities of strip footings located on the ground surface for the same soil properties (unit weight and friction angle). In addition to revisiting the terms in the traditional bearing capacity equation and proposing new, improved relationships, we shall also propose a different form of the bearing capacity equation, a simpler form, that does not require an assumption of independence of the self-weight and surcharge effects. This new form of the bearing capacity equation consists of one term instead of two.

CALCULATION OF LIMIT BEARING CAPACITY USING LIMIT ANALYSIS

Limit analysis: background

From the time Hill (1951) and Drucker *et al.* (1951,1952) published their ground-breaking lower and upper-bound theorems of plasticity theory, on which limit analysis is based, it was apparent that limit analysis would be a tool that would provide important insights into the bearing capacity problem and other stability applications. However, the numerical techniques required for finding very close lower and upper bounds on collapse loads, thus accurately estimating the collapse loads themselves, were not available until very recently.

Table 1. Commonly used expressions for shape factors

	q_0 term	γ term
Meyerhof (1963)	$s_q = 1 + 0{\cdot}1N\dfrac{B}{L}$	$s_\gamma = 1 + 0{\cdot}1N\dfrac{B}{L}$
Brinch Hansen (1970)	$s_q = 1 + \dfrac{B}{L}\sin\phi$	$s_\gamma = 1 - 0{\cdot}4\dfrac{B}{L} \geqslant 0{\cdot}6$
Vesic (1973)	$s_q = 1 + \dfrac{B}{L}\tan\phi$	$s_\gamma = 1 - 0{\cdot}4\dfrac{B}{L} \geqslant 0{\cdot}6$

N = flow number = $\tan^2(45+\phi/2)$.

Table 2. Commonly used expressions for depth factors

	q_0 term	γ term
Meyerhof (1963)	$d_q = 1 + 0{\cdot}1\sqrt{N}\dfrac{D}{B}$	$d_\gamma = 1 + 0{\cdot}1\sqrt{N}\dfrac{D}{B}$
Brinch Hansen (1970) and Vesic (1973)	$D/B \leqslant 1$: $d_q = 1 + 2\tan\phi(1 - \sin\phi)^2\dfrac{D}{B}$ $D/B > 1$ $d_q = 1 + 2\tan\phi(1 - \sin\phi)^2\tan^{-1}\dfrac{D}{B}$	$d_\gamma = 1$

N = flow number = $\tan^2(45+\phi/2)$.

Limit analysis takes advantage of the lower- and upper-bound theorems of plasticity theory to bound the rigorous solution to a stability problem from below and above. The theorems are based on the principle of maximum power

dissipation of plasticity theory, which is valid for soil following an associated flow rule. If soil does not follow an associated flow rule (the case with sands), the bearing capacity values from limit analysis may be too high. The focus of the present paper is on frictional soils following an associated flow rule. However, for relative quantities (such as shape and depth factors), the results produced by limit analysis can be considered reasonable estimates of the quantities for sands.

$$\boldsymbol{\sigma}^l = \{\sigma^l_{11} \; \sigma^l_{22} \; \sigma^l_{33} \; \sigma^l_{12} \; \sigma^l_{23} \; \sigma^l_{31}\}^{\mathsf{T}}; \quad l = 1, ..., 4$$

(a)

$$\boldsymbol{\sigma}^e = \{\sigma^e_{11} \; \sigma^e_{22} \; \sigma^e_{33} \; \sigma^e_{12} \; \sigma^e_{23} \; \sigma^e_{31}\}^{\mathsf{T}}$$
$$\mathbf{u}^l = \{u^l_1 u^l_2 u^l_3\}^{\mathsf{T}}; \; l = 1, ..., 4$$

(b)
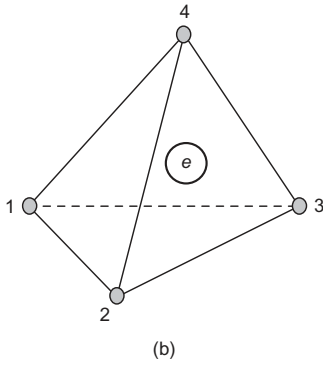
Fig. 1. Three-dimensional finite elements for: (a) lower-bound analysis; (b) upper-bound analysis

Discrete formulation of lower-bound theorem

The objective of a lower-bound calculation is to find a stress field σ_{ij} that satisfies equilibrium throughout the soil
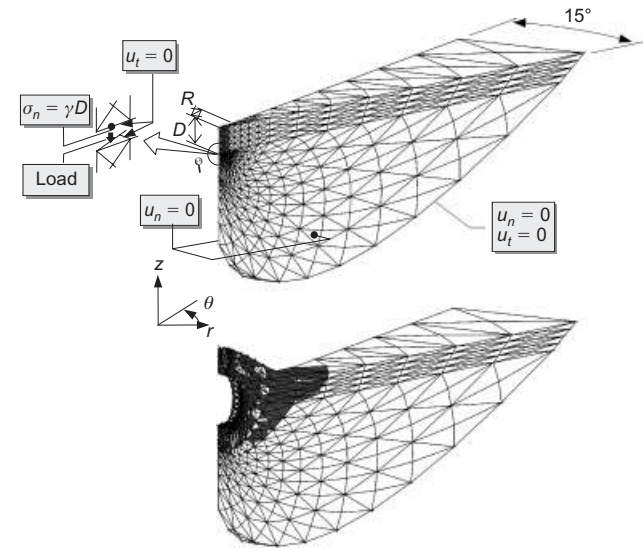

Fig. 3. Typical upper-bound mesh and deformation pattern for circular footings

Fig. 2. Typical lower-bound mesh and plasticity zones for circular footings
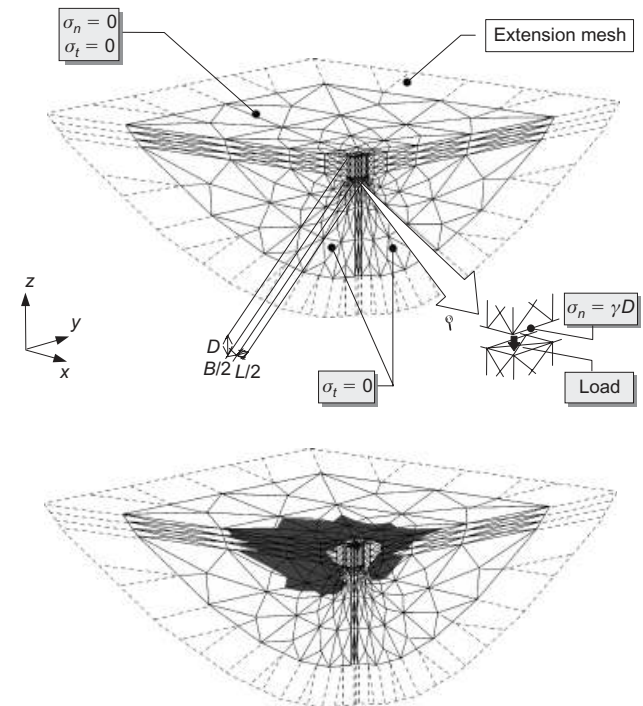
Fig. 4. Typical lower-bound mesh and plasticity zones for rectangular footings
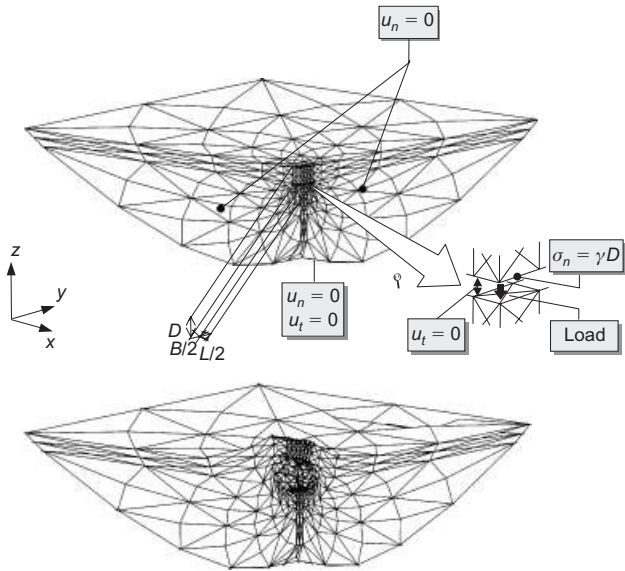
Fig. 5. Typical upper-bound mesh and deformation pattern for rectangular footings

mass, balances the prescribed surface tractions, nowhere violates the yield criterion, and maximises Q, given in the general case by

$$Q = \int_S \mathbf{T}\,\mathrm{d}S + \int_V \mathbf{X}\,\mathrm{d}V \tag{8}$$

where $\mathbf{T}$ and $\mathbf{X}$ are, respectively, the surface tractions and body forces. In our analyses, body forces (soil weight) are prescribed: therefore equation (8) reduces to the first integral only.

The numerical implementation of the limit analysis theorems usually proceeds by discretising the continuum into a set of finite elements and then using mathematical programming techniques to solve the resulting optimisation problem. The choice of finite elements that can be employed to guarantee a rigorous lower-bound numerical formulation is rather limited. They must be linear stress elements. Additionally, consideration of equilibrium of any two elements sharing a face does not lead to a requirement of continuity of the normal stress in a direction parallel to the shared face (Fig. 1(a)). In the present analysis, these stress discontinu-

(a)

(b)

(c)

Fig. 6. Lower-bound mesh and plasticity zones for strip footing with: (a) $D/B = 0\cdot2$; (b) $D/B = 1\cdot0$; (c) $D/B = 2\cdot0$

ities are placed between all elements. If D is the problem dimensionality, then there are $D + 1$ nodes in each element, and each node is associated with a $(D^2 + D)/2$-dimensional vector of stress variables $\{\sigma_{ij}\}$, $i = 1, \ldots, D$; $j = i, \ldots, D$. These stresses are taken as the problem variables.

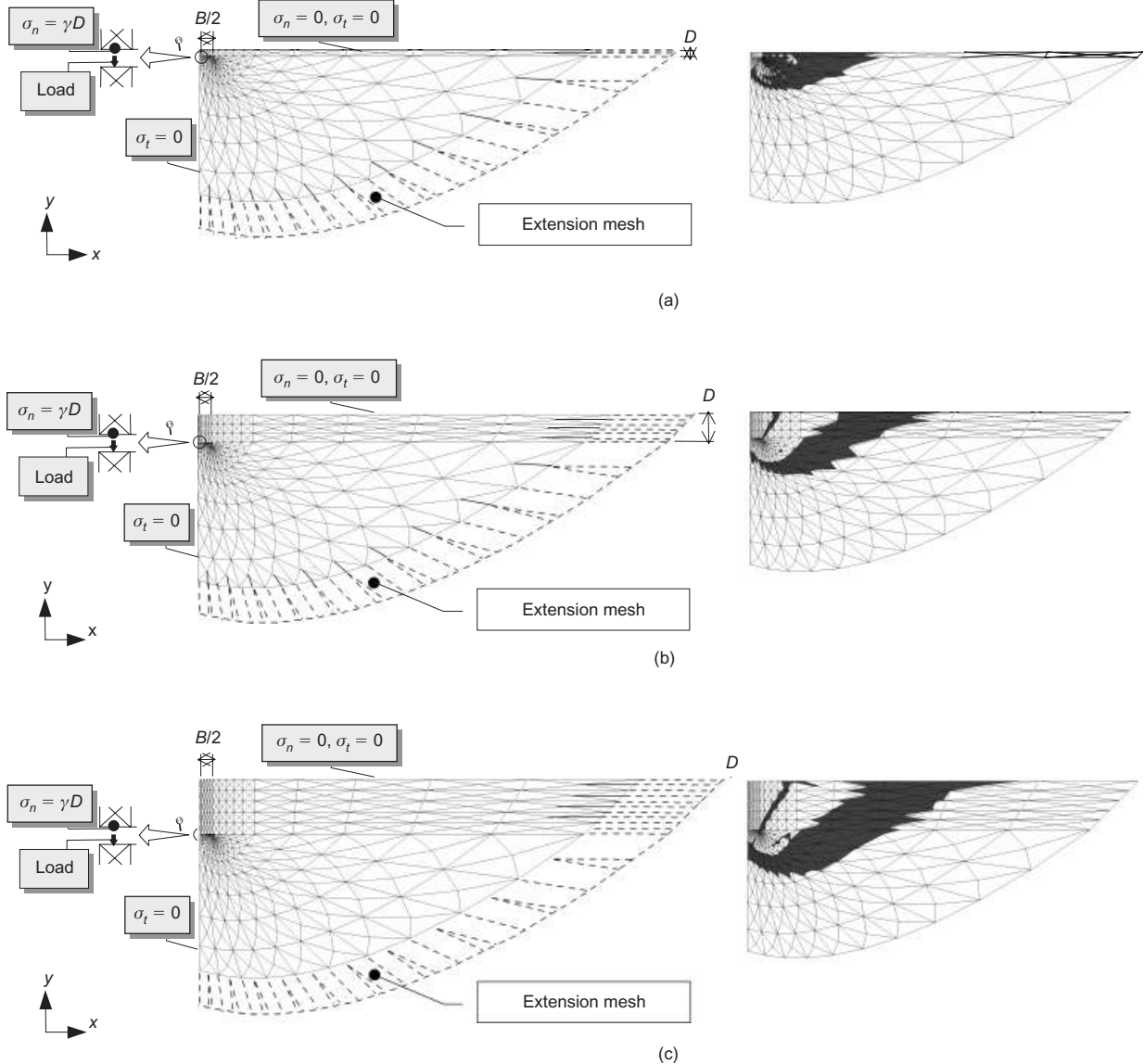A detailed description of the numerical formulation of the lower-bound theorem utilised in the present study is beyond the scope of the paper, but can be found in Lyamin (1999) and Lyamin & Sloan (2002a).

Discrete formulation of upper-bound theorem

The objective of an upper-bound calculation is to find a velocity distribution **u** that satisfies compatibility, the flow rule and the velocity boundary conditions, and which minimises the internal power dissipation less the rate of work done by prescribed external forces:

$$W_1 = \int_V \boldsymbol{\sigma} \dot{\boldsymbol{\varepsilon}} \, dV - \int_S \mathbf{T}_p^T \mathbf{u} \, dS - \int_V \mathbf{X}_p^T \mathbf{u} \, dV \tag{9}$$

An upper-bound estimate on the true collapse load can be obtained by equating W_1 to the rate of work done by all other external loads, given by

$$W_2 = \int_S \mathbf{T}^T \mathbf{u} \, dS + \int_V \mathbf{X}^T \mathbf{u} \, dV \tag{10}$$

For a cohesionless soil there is no energy dissipation. In a bearing capacity problem, this means that the bearing capacity comes entirely from the self-weight of the soil. Additionally, minimisation of W_1 implies maximisation of W_2, which is due entirely to the tractions applied on the soil mass by the footing.

In contrast to the lower-bound formulation, there is more than one type of finite element that will enforce rigorous upper-bound calculations (e.g. Yu *et al.*, 1994; Makrodimo-poulos & Martin, 2005). In the present work, we use the simplex finite element illustrated in Fig. 1(b). Kinematically admissible velocity discontinuities are permitted at all interfaces between adjacent elements. If D is the dimensionality of the problem, then there are $D + 1$ nodes in the element, and each node is associated with a D-dimensional vector of velocity variables $\{u_i\}$, $i = 1, \ldots, D$. These, together with a $(D^2 + D)/2$-dimensional vector of elemental stresses $\{\sigma_{ij}\}$, $i = 1, \ldots, D$; $j = i, \ldots, D$, and a $2(D - 1)$-dimensional vector of discontinuity velocity variables v^d are taken as the problem variables.

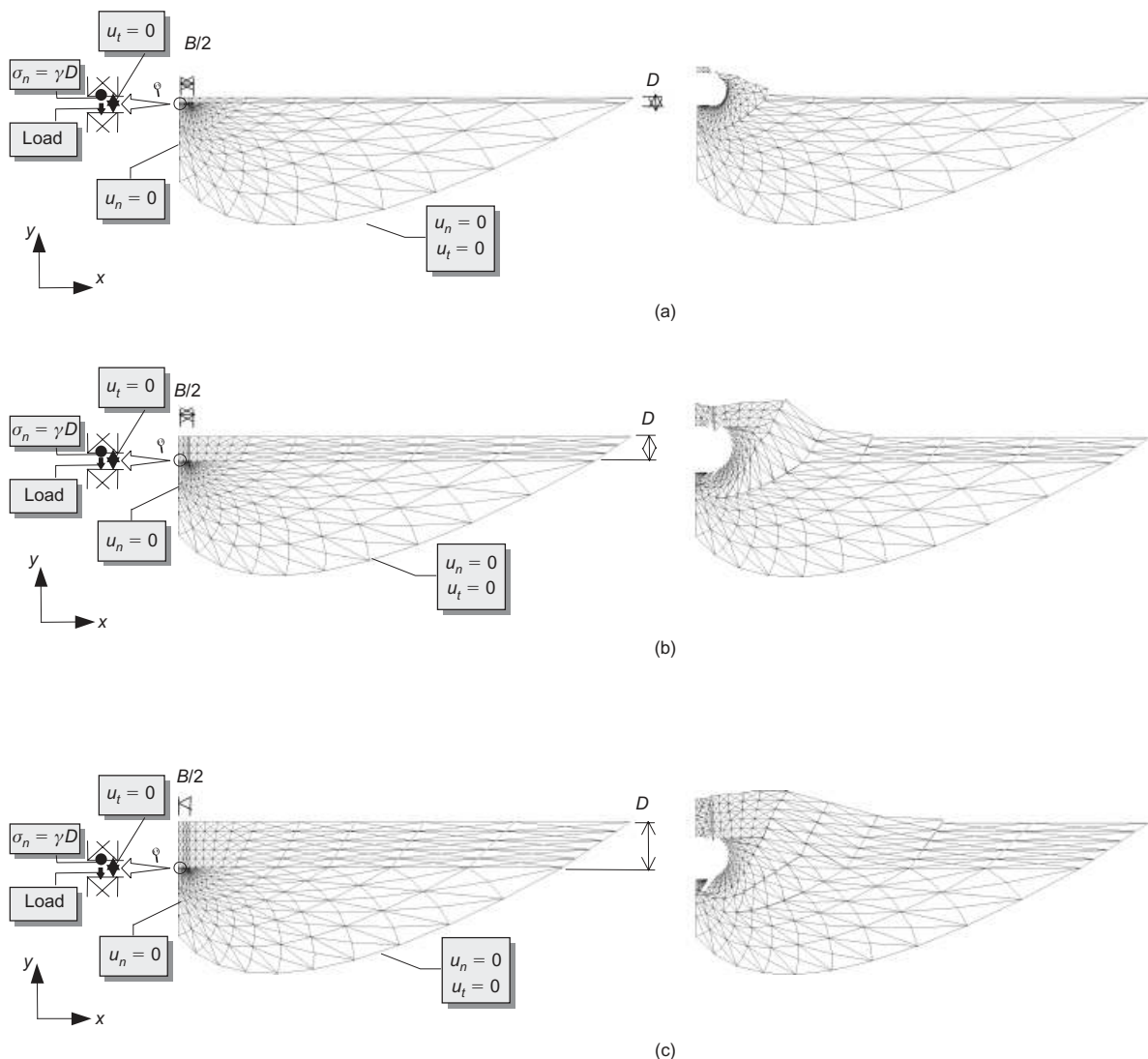A comprehensive description of the dimensionally independent upper-bound formulation (suitable for cohesive-

Fig. 7. Upper-bound mesh and deformation pattern for strip footing with: (a) $D/B = 0\cdot2$; (b) $D/B = 1\cdot0$; (c) $D/B = 2\cdot0$

frictional materials) used to carry out computations for this research is given in Lyamin & Sloan (2002b), Lyamin *et al.* (2005) and Krabbenhøft *et al.* (2005).

TYPICAL MESHES FOR EMBEDDED FOOTING PROBLEM

To increase the accuracy of the computed depth and shape factors for 3D footings, the symmetry inherent in all of these problems is fully exploited. This means that only 15°, 45° and 90° sectors are discretised for the circular, square and rectangular footings respectively, as shown in Figs 2–7. These plots also show the boundary conditions adopted in the various analyses and resultant plasticity zones (shown as shaded in the figures) and deformation patterns. The 15° sector for circular footings has been used to minimise computation time. A slice with such a thickness can be discretised using only one layer of well-shaped elements, while keeping the error in geometry representation below 1% (which is approximately five times less than the accuracy of the predicted collapse load, as we shall see later).

For the lower-bound meshes, special extension elements are included to extend the stress field over the semi-infinite domain (thus guaranteeing that the solutions obtained are rigorous lower bounds on the true solutions; Pastor, 1978). To model the embedded conditions properly, the space above the footing was filled with soil. At the same time, the model includes a gap between the top of the footing and this fill; this gap is supported by normal hydrostatic pressure, as shown in the enlarged diagrams of Figs 2–7. Rough condi-

tions are applied at the top and bottom of the footing by prescribing zero tangential velocity for upper-bound calculations and specifying no particular shear stresses for lower-bound calculations (that is, the yield criterion is operative between the footing and the soil in the same way as it is operative within the soil). This modelling strategy is geometrically simple, producing a result that is close to the desired quantity (pure unit base resistance) with only a slight conservative bias when compared with other possible modelling options, shown in Fig. 8.

In order to illustrate the differences between results from the different options, we performed a model comparison study, which is summarised in Table 3. For each option, the lower (LB), upper (UB) and average (Avg) values of collapse pressure were computed using FE meshes similar to those shown in Figs 6 and 7. From the results presented in Table 3, it is apparent that a simple 'rigid-block' model is on the unsafe side when 'rough' walls are assumed, and is too conservative when 'smooth' walls are assumed, when compared with realistically shaped footings. On the other hand, the 'rigid-plate' model with hydrostatically supported soil above the plate is safe for all considered D/B ratios and has the lowest geometric complexity (which is especially helpful in modelling 3D cases). Note, however, that the differences between the results of all the analyses are not large, even for the maximum D/B value considered in the calculations. The difference between all considered footing geometries and wall/soil interface conditions (for a rough base in all cases) is not greater than 14%. If we exclude the 'rigid-
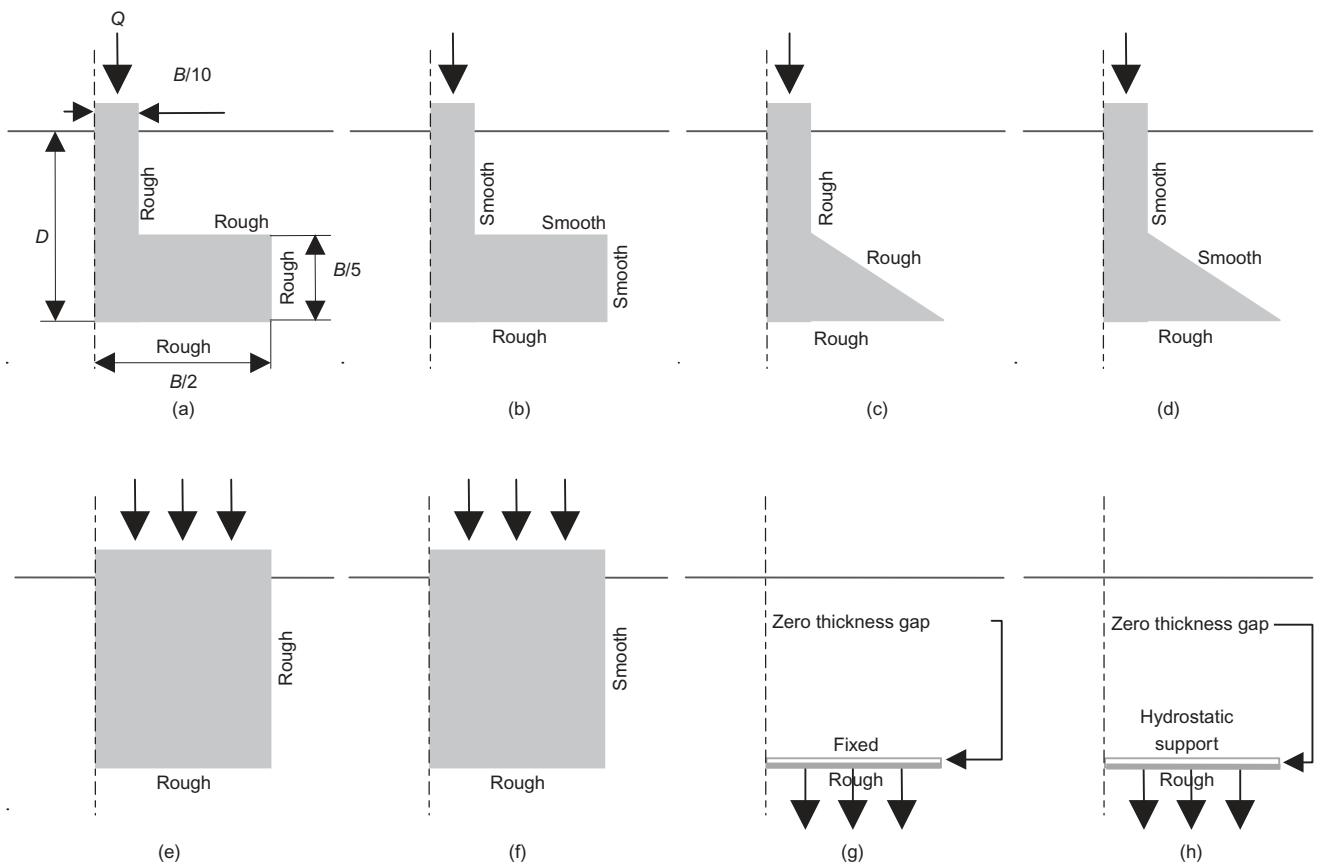

Fig. 8. Modelling options for embedded 2D footing: (a) T-bar, rough base, rough walls; (b) T-bar, rough base, smooth walls; (c) T-cone, rough base, rough walls; (d) T-cone, rough base, smooth walls; (e) block, rough base, rough walls; (f) block, rough base, smooth walls; (g) plate, rough base, fixed top; (h) plate, rough base, hydrostatically supported top

Table 3. Bearing capacities of different 2D models of embedded footing

$\frac{D}{B}$	T-bar footing						T-cone footing						Rigid block footing						Rigid plate (fixed top)			Rigid plate (top support)		
	Rough walls			Smooth walls			Rough walls			Smooth walls			Rough walls			Smooth walls								
	LB	UB	Avg	LB	UB	Avg	LB	UB	Avr	LB	UB	Avg	LB	UB	Avg	LB	UB	Avg	LB	UB	Avg	LB	UB	Avg
0·4													77·1	85·6	81·4	75·7	83·3	79·5	77·1	84·8	80·9	76·5	84·0	80·2
1·0	134·1	150·2	142·1	132·2	147·6	139·9	133·4	148·4	140·9	133·3	148·3	140·8	138·1	154·8	146·5	130·0	144·7	137·3	134·3	149·3	141·8	132·0	146·6	139·3
2·0	241·7	271·0	256·3	236·4	262·7	249·6	241·6	269·2	255·4	237·4	263·1	250·3	258·8	289·3	274·1	228·9	253·8	241·4	239·5	265·0	252·3	232·9	257·9	245·4

block' model, this figure drops to just 5% for the maximum D/B ratio considered.

DETERMINATION OF THE TRADITIONAL BEARING CAPACITY EQUATION TERMS
Range of conditions considered in the calculations

Our goal in this section is to generate equations for shape and depth factors that will perform the same function as the equations in Tables 1 and 2, but will do so with greater accuracy. The range of friction angles of sands is from roughly 27° to about 45° for square and circular footings, and from 27° to about 50° for strip footings, to which plane-strain friction angles apply. Accordingly, the frictional soils considered in our calculations have $\phi = 25°$, 30°, 35°, 40° and 45°.

We are interested in both circular and square footings. In practice, most rectangular footings have L/B of no more than 4, where L and B are the two plan dimensions of the footing. Accordingly, our calculations are for footings with $L/B = 1$, 2, 3 and 4. The maximum embedment for shallow foundations is typically taken as $D = B$. We more liberally established 2 as the upper limit of the D/B range considered in our calculations. The embedment ratios we considered were 0·1, 0·2, 0·4, 0·6, 0·8, 1 and 2.

Determination of N_γ

The very first step in this process of analysis of the bearing capacity equation is the determination of N_γ, which requires the determination of lower and upper bounds on the bearing capacity of a strip footing on the surface of a frictional soil. Equation (1) is rewritten for this case as

$$q_{bL} = \frac{1}{2}\gamma B N_\gamma \qquad (11)$$

Calculations were done with $\gamma = 1$ and $B = 2$ so that q_{bL} resulted numerically equal to N_γ. The lower- and upper-bound values of N_γ calculated in this way using limit analysis are shown in Table 4 and Fig. 9, which also show the values calculated using equations (5), (6) and (7). For completeness, the table also shows the value of N_q for each friction angle. It can be seen that the values of N_γ calculated using equation (5) fall between the lower and upper bounds on N_γ for ϕ values lower than 40° and then fall below the lower bound for $\phi \geqslant 40°$. Values of N_γ calculated using equation (7) fall within the range determined by lower- and upper-bound solutions for all ϕ values of interest. On the other hand, the N_γ values calculated using equation (6) are too high. So this equation, the Caquot & Kerisel (1953) equation, is not correct, and its use should be discouraged.

Determination of the depth factors

The depth factor d_γ was taken as 1 by both Vesic (1973) and Brinch Hansen (1970), as seen in Table 2. Conceptually, a value of $d_\gamma = 1$ means that the N_γ term refers only to the slip mechanism that forms below the base of the footing. This means that the effects of the portion of the mechanism extending above the base of the footing are fully captured by the depth factor d_q. In this section, consistent with what has traditionally been done, we take $d_\gamma = 1$ as well. Later in the paper we shall present an alternative way to account for embedment of the footing.

For the determination of d_q, we consider a strip footing at depth. For this case, equation (1) becomes

Table 4. Values of N_q and N_γ calculated using limit analysis and equations (5), (6) and (7).

ϕ	N_q	N_γ			N_γ (Martin)	N_γ (LB)	N_γ (UB)	Error: %	$N_{\gamma,w}$	Error: %
		Equation (5)	Equation (6)	Equation (7)						
25°	10·66	6·76	10·88	6·49	6·49	6·44	7·09	4·80	6·72	3·57
30°	18·40	15·07	22·40	14·75	14·75	14·57	15·90	4·36	15·51	5·18
35°	33·30	33·92	48·03	34·48	34·48	33·81	36·98	4·48	35·01	1·54
40°	64·20	79·54	109·41	85·47	85·57	82·29	91·86	5·50	89·94	5·10
45°	134·87	200·81	271·75	234·2	234·21	221·71	255·44	7·07	242·96	3·74
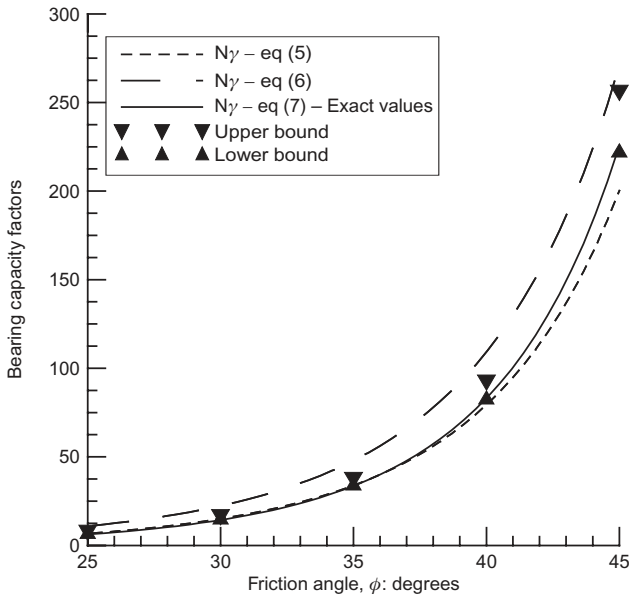
Fig. 9. Bearing capacity factor N_γ from upper- and lower-bound analyses and from equations due to Brinch Hansen (1970) and Caquot & Kerisel (1953)

$$q_{bL} = d_q q_0 N_q + 0.5\gamma B N_\gamma$$

$$= d_q \gamma D N_q + 0.5\gamma B N_\gamma \qquad (12)$$

The lower and upper bounds on the second term on the right side of (12)—and indeed the nearly exact value of it—are known, as discussed earlier. The corresponding values of d_q can then be calculated from equation (12), rewritten as

$$d_q = \frac{q_{bL} - 0.5\gamma B N_\gamma}{q_0 N_q} \qquad (13)$$

The results of these calculations, given in Table 5, show clearly that the depth factor d_q does not approach 1 when $D/B \to 0$, as would be suggested by the expressions given in Table 2. On the contrary, it increases with decreasing D/B. This fact can be explained by the inadequacy of the logic of superposition and segregation of the different contributions to bearing capacity. Indeed, the theory of the depth factor d_q is that it would correct for the shear strength of the soil located above the level of the footing base, which disappears upon the replacement of the overburden soil by a surcharge. The reality of the depth factor d_q, computed using equation (13), is that it accumulates two contributions. The first contribution is the intended one: the contribution of the shear strength of the soil

Fig. 10. Illustration of difference in work done by external forces in two cases: (a) equivalent surcharge used to replace soil above base of footing; (b) footing modelled as an embedded footing

Table 5. Depth factor d_q (obtained from weighted average of lower and upper bounds on strip footing bearing capacity) for $D = 0.1$ to $2B$ and $\phi = 25-45°$

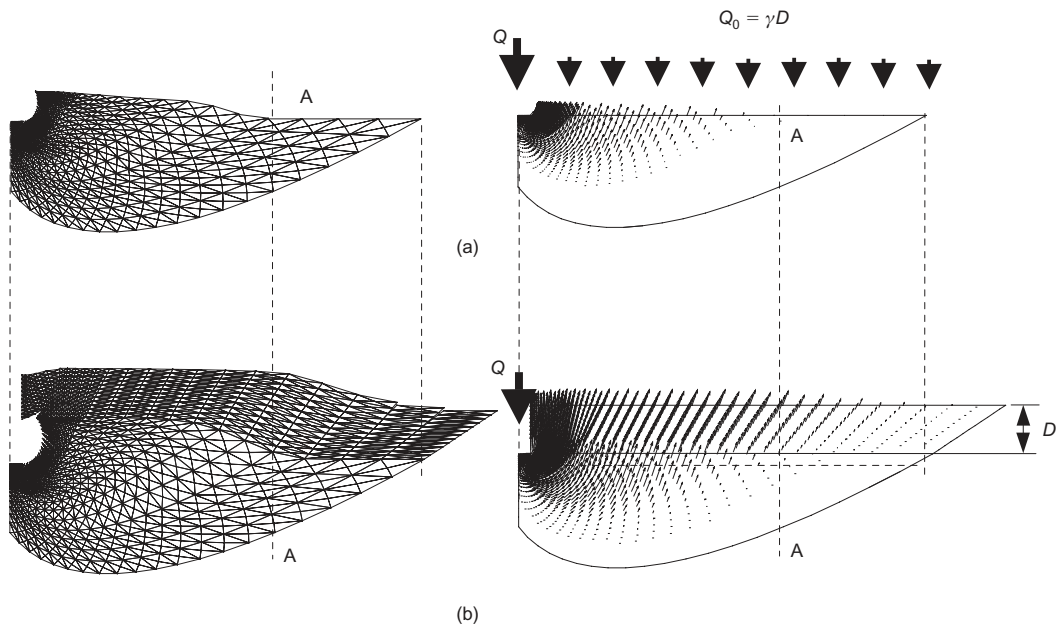| ϕ	D/B	q_{bL} (LB)	q_{bL} (UB)	q_{bL}	q_0	$q_0 N_q$	$0.5\gamma B N_\gamma$	d_q	Error: %
25°	0·1	10·62	11·07	10·65	0·2	2·13	6·49	1·95	2·11
	0·2	13·90	14·41	13·94	0·4	4·26	6·49	1·75	1·83
	0·4	19·99	20·73	20·05	0·8	8·53	6·49	1·59	1·85
	0·6	25·92	26·87	25·99	1·2	12·79	6·49	1·52	1·83
	0·8	31·93	33·16	32·02	1·6	17·06	6·49	1·50	1·92
	1·0	38·08	39·67	38·20	2·0	21·32	6·49	1·49	2·08
	2·0	70·85	73·95	71·09	4·0	42·65	6·49	1·51	2·18
30°	0·1	21·90	23·07	22·06	0·2	3·68	14·75	1·99	2·65
	0·2	27·59	28·88	27·76	0·4	7·36	14·75	1·77	2·32
	0·4	38·07	39·91	38·32	0·8	14·72	14·75	1·60	2·40
	0·6	48·37	50·67	48·68	1·2	22·08	14·75	1·54	2·36
	0·8	58·76	61·47	59·13	1·6	29·44	14·75	1·51	2·29
	1·0	69·21	72·81	69·70	2·0	36·80	14·75	1·49	2·58
	2·0	125·44	132·52	126·40	4·0	73·60	14·75	1·52	2·80
35°	0·1	46·99	50·04	47·63	0·2	6·66	34·48	1·98	3·20
	0·2	57·29	60·89	58·05	0·4	13·32	34·48	1·77	3·10
	0·4	76·49	81·09	77·46	0·8	26·64	34·48	1·61	2·97
	0·6	95·11	100·74	96·30	1·2	39·96	34·48	1·55	2·92
	0·8	113·46	120·65	114·98	1·6	53·27	34·48	1·51	3·13
	1·0	132·07	140·95	133·95	2·0	66·59	34·48	1·49	3·31
	2·0	232·93	248·15	236·15	4·0	133·18	34·48	1·51	3·22
40°	0·1	108·09	117·84	111·43	0·2	12·84	85·57	2·01	4·37
	0·2	128·53	139·60	132·32	0·4	25·68	85·57	1·82	4·18
	0·4	165·62	179·30	170·31	0·8	51·36	85·57	1·65	4·02
	0·6	201·32	217·82	206·98	1·2	77·03	85·57	1·58	3·99
	0·8	237·00	256·76	243·77	1·6	102·71	85·57	1·54	4·05
	1·0	273·13	295·84	280·91	2·0	128·39	85·57	1·52	4·04
	2·0	463·99	499·86	476·28	4·0	256·78	85·57	1·52	3·77
45°	0·1	277·45	312·38	290·39	0·2	26·97	234·21	2·08	6·01
	0·2	321·10	360·05	335·53	0·4	53·95	234·21	1·88	5·80
	0·4	401·50	447·54	418·56	0·8	107·90	234·21	1·71	5·50
	0·6	479·00	531·41	498·42	1·2	161·85	234·21	1·63	5·26
	0·8	555·46	614·58	577·37	1·6	215·80	234·21	1·59	5·12
	1·0	631·77	696·15	655·63	2·0	269·75	234·21	1·56	4·91
	2·0	1019·70	1117·08	1055·79	4·0	539·50	234·21	1·52	4·61
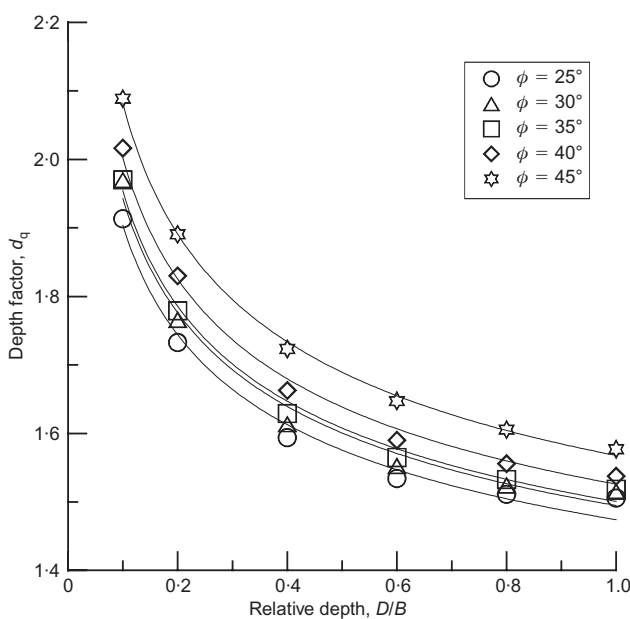
Fig. 11. Depth factor d_q against depth for various friction angles

located above the level of the footing base, which is lost upon its replacement by an equivalent surcharge. The second contribution results from the fact that replacing the soil above the footing base by an equivalent surcharge produces a different response of the soil below the footing base. Note that this is contrary to the assumption that the response of the soil below the footing base is independent of what happens above it (which is the logic behind making $d_\gamma = 1$). Fig. 10 shows, using upper-bound calculations, that the rate of work done by displacing the soil above the level of an embedded footing must be greater than the rate of work done against an equivalent surface footing (i.e. the footing plus a surcharge equivalent to the overburden pressure associated with the embedment). This is seen by the larger extent of the collapse mechanism in the presence of soil above the footing base compared with that for an equivalent surface footing. To visualise this, one can compare Fig. 10(a) and Fig. 10(b). It can be seen from this comparison that no displacement of the soil is occurring on the right side of line A–A for the case in which a surcharge load is used: so A–A marks the boundary of the collapse mechanism in that case. However, there is considerable displacement of soil to the right of A–A for the case of the embedded footing. So the fact that there is a soil-on-soil interaction at the

Table 6. Lower and upper bounds on shape factors and their weighted averages.

Circular footing

ϕ	N_γ	$s_\gamma N_\gamma$ (LB)	s_γ (LB)	$s_\gamma N_\gamma$ (UB)	s_γ (UB)	ΔUB/ΔLB	w (LB)	w (UB)	$s_\gamma N_{\gamma,\mathrm{w}}$	$s_{\gamma,\mathrm{w}}$
25°	6·49	5·65	0·87	8·26	1·27	3·57	0·78	0·22	6·22	0·96
30°	14·75	14·10	0·96	19·84	1·35	2·69	0·73	0·27	15·65	1·06
35°	34·48	37·18	1·08	52·51	1·52	2·69	0·73	0·27	41·33	1·20
40°	85·57	106·60	1·25	157·21	1·84	2·41	0·71	0·29	121·45	1·42
45°	234·21	338·00	1·44	539·22	2·30	2·31	0·70	0·30	398·80	1·70

Square footing

ϕ	N_γ	$s_\gamma N_\gamma$ (LB)	s_γ (LB)	$s_\gamma N_\gamma$ (UB)	s_γ (UB)	ΔUB/ΔLB	w (LB)	w (UB)	$s_\gamma N_{\gamma,\mathrm{w}}$	$s_{\gamma,\mathrm{w}}$
25°	6·49	5·10	0·79	9·05	1·39	4·15	0·81	0·19	5·87	0·90
30°	14·75	12·67	0·86	21·82	1·48	4·03	0·80	0·20	14·49	0·98
35°	34·48	32·96	0·96	58·60	1·70	3·54	0·78	0·22	38·61	1·12
40°	85·57	91·04	1·06	184·73	2·16	3·30	0·77	0·23	112·84	1·32
45°	234·21	277·00	1·18	683·09	2·92	3·63	0·78	0·22	364·79	1·56

Rectangular footing, $L/B = 1\cdot2$

ϕ	N_γ	$s_\gamma N_\gamma$ (LB)	s_γ (LB)	$s_\gamma N_\gamma$ (UB)	s_γ (UB)	ΔUB/ΔLB	w (LB)	w (UB)	$s_\gamma N_{\gamma,\mathrm{w}}$	$s_{\gamma,\mathrm{w}}$
25°	6·49	4·77	0·73	13·60	2·10	6·80	0·87	0·13	5·90	0·91
30°	14·75	11·57	0·78	30·31	2·05	5·22	0·84	0·16	14·58	0·99
35°	34·48	28·48	0·83	79·11	2·29	3·93	0·80	0·20	38·75	1·12
40°	85·57	71·91	0·84	268·98	3·14	4·44	0·82	0·18	108·14	1·26
45°	234·21	194·70	0·83	1013·72	4·33	3·97	0·80	0·20	359·59	1·54

Rectangular footing, $L/B = 2$

ϕ	N_γ	$s_\gamma N_\gamma$ (LB)	s_γ (LB)	$s_\gamma N_\gamma$ (UB)	s_γ (UB)	ΔUB/ΔLB	w (LB)	w (UB)	$s_\gamma N_{\gamma,\mathrm{w}}$	$s_{\gamma,\mathrm{w}}$
25°	6·49	5·10	0·79	12·47	1·92	5·99	0·86	0·14	6·15	0·95
30°	14·75	12·10	0·82	27·57	1·87	4·44	0·82	0·18	14·94	1·01
35°	34·48	28·87	0·84	71·77	2·08	3·78	0·79	0·21	37·84	1·10
40°	85·57	71·10	0·83	233·92	2·73	4·60	0·82	0·18	100·19	1·17
45°	234·21	189·60	0·81	870·00	3·71	5·38	0·84	0·16	296·19	1·26

Rectangular footing, $L/B = 3$

ϕ	N_γ	$s_\gamma N_\gamma$ (LB)	s_γ (LB)	$s_\gamma N_\gamma$ (UB)	s_γ (UB)	ΔUB/ΔLB	w (LB)	w (UB)	$s_\gamma N_{\gamma,\mathrm{w}}$	$s_{\gamma,\mathrm{w}}$
25°	6·49	5·16	0·80	11·74	1·81	4·85	0·83	0·17	6·28	0·97
30°	14·75	12·08	0·82	26·13	1·77	3·85	0·79	0·21	14·98	1·02
35°	34·48	28·11	0·82	68·69	1·99	3·65	0·78	0·22	36·84	1·07
40°	85·57	67·36	0·79	214·76	2·51	4·45	0·82	0·18	94·41	1·10
45°	234·21	174·90	0·75	786·85	3·36	5·10	0·84	0·16	275·26	1·18

Rectangular footing, $L/B = 4$

ϕ	N_γ	$s_\gamma N_\gamma$ (LB)	s_γ (LB)	$s_\gamma N_\gamma$ (UB)	s_γ (UB)	ΔUB/ΔLB	w (LB)	w (UB)	$s_\gamma N_{\gamma,\mathrm{w}}$	$s_{\gamma,\mathrm{w}}$
25°	6·49	5·15	0·79	11·30	1·74	3·97	0·80	0·20	6·39	0·98
30°	14·75	11·98	0·81	25·20	1·71	3·40	0·77	0·23	14·98	1·02
35°	34·48	27·50	0·80	67·50	1·96	3·75	0·79	0·21	35·92	1·04
40°	85·57	64·78	0·76	203·40	2·38	4·17	0·81	0·19	91·58	1·07
45°	234·21	165·00	0·70	739·00	3·16	5·19	0·84	0·16	257·66	1·10

level of the base of the footing, as opposed to simply a surcharge applied on the soil surface with a footing also resting on the soil surface, does have an impact on what happens below the footing base level. When that is ignored by making $d_\gamma = 1$, the effects appear in the value of d_q.

The depth factor d_q is plotted in Fig. 11 with respect to the depth of embedment for the five friction angles examined: 25°, 30°, 35°, 40° and 45°. The following equation fits

well the numbers for $\phi = 25°$ to 45° in the D/B range from 0 to 2.

$$d_q = 1 + (0\cdot0036\phi + 0\cdot393)\left(\frac{D}{B}\right)^{-0\cdot27} \tag{14}$$

In this and all subsequent equations presented in the paper it is assumed that the angle of soil internal friction, ϕ, is expressed in degrees.
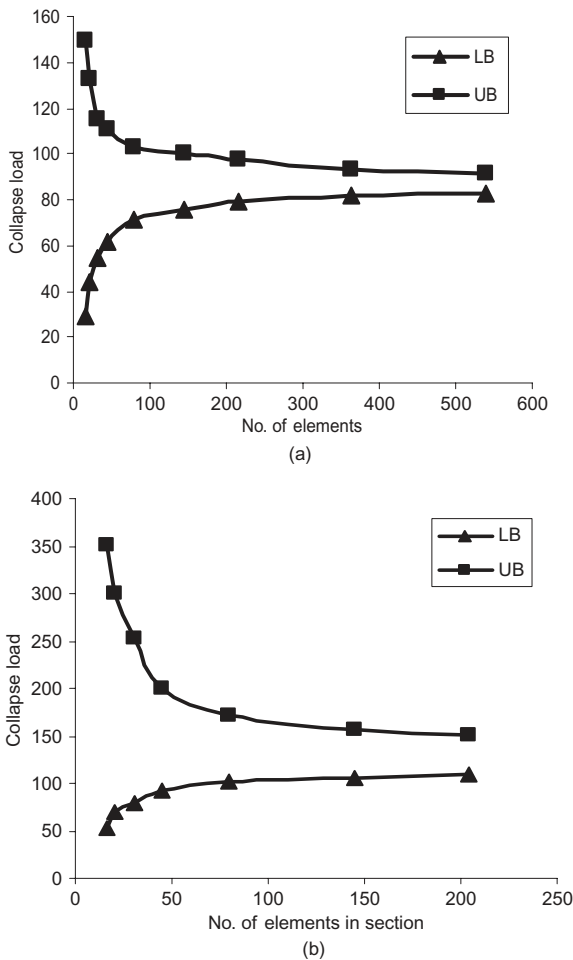
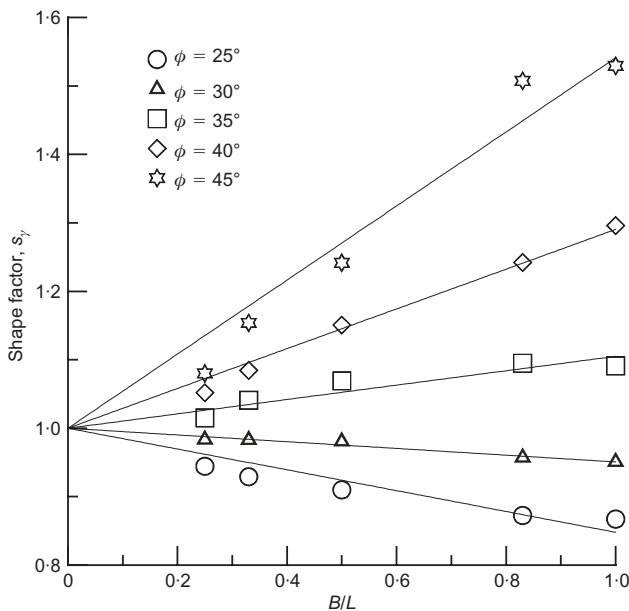**Fig. 12. Convergence for: (a) strip footings; (b) circular footings**

Fig. 13. Variation of shape factor s_γ for surface footings with respect to B/L

Determination of s_γ

For a square, circular or rectangular footing on the surface of a soil deposit, equation (1) becomes

$$q_{bL} = 0.5\gamma B s_\gamma N_\gamma \qquad (15)$$

Given that $0.5\gamma B = 1$ in our calculations, the calculated bounds on q_{bL} are bounds on $s_\gamma N_\gamma$. These values are shown in Table 6. The lower-bound s_γ is obtained by dividing the lower-bound $s_\gamma N_\gamma$ by the corresponding N_γ value from Martin (2005), shown in the second column of the table (and approximated by equation (7)). The bounds on s_γ are also given in Table 6.

Taking the average of the upper and lower bounds as our best estimate of s_γ would be appropriate if the lower and upper bounds converged to a common value at the same rate with increasing mesh refinement. It was observed, however, particularly for rectangular footings (for which computation accuracy drops significantly with increasing values of L/B because of the coarser mesh that must be used), that the convergence rates are different for lower- and upper-bound calculations. A convergence study was performed for each of the 3D shapes considered for footings in the present paper by using progressively finer meshes. The convergence rates are approximately the same for lower- and upper-bound computations for the plane-strain case, as shown in Fig. 12(a), but the convergence rates for bounds on the bearing capacity of footings with finite values of L are significantly different (see Fig. 12(b)). This means that taking the average of the two bounds does not give the best estimate of s_γ, which is obtained instead from the asymptotes computed for the lower- and upper-bound solutions. If, say LB_1 and LB_2 are two lower-bound estimates on some quantity obtained with two different FE meshes, and UB_1 and UB_2 are two upper-bound solutions from two meshes like the two lower-bound meshes, then the ratio of convergence rates of bounding solutions can be written as

$$\alpha = \frac{\Delta UB}{\Delta LB} = \frac{UB_1 - UB_2}{LB_2 - LB_1}$$

Given that information, the point of intersection of LB and UB plots (which we may call a weighted-average approximation to the collapse load) can be estimated as

$$PI = w_{LB}LB_1 + w_{UB}UB_1$$

where

$$w_{LB} = \frac{\alpha}{1 + \alpha}, \quad w_{UB} = \frac{1}{1 + \alpha}$$

To assess the level of accuracy that can be expected from this approach, N_γ was calculated using the above formula and coarse meshes with the same pattern as the cross-sections of the 3D meshes used for circular and rectangular footings. The results of this test are presented in the last two columns of Table 4. The coarse meshes used in the N_γ computations result in a wide gap between bounds (as observed in some of the 3D calculations), but the weighted average estimates, $N_{\gamma,w}$, are quite close to the exact values of N_γ.

Figure 13 shows the results of calculations for surface footings. These results suggest that there are no simple generalisations, based on physical rationalisations, as to what the shape factor s_γ should be. It can be greater or less than 1, and increase or decrease with increasing B/L. Note that s_γ is both less than 1 and decreases with increasing B/L for $\phi = 25°$ and $\phi = 30°$, whereas it is greater than 1 and increases with increasing B/L for $\phi = 35°-45°$ (which are the cases of greater interest in practice). Note also that the value of ϕ that would lead to $s_\gamma = 1$ for all values of B/L is slightly greater than 30°. Using the Martin (2005) N_γ values as a reference, our shape factors for $\phi = 35°-45°$ are 15–20% lower than the values of Erickson & Drescher (2002), obtained using FLAC. A final interesting observation is that the variation of s_γ with B/L is essentially linear for all ϕ values considered. Zhu & Michalowski (2005) also observed

Table 7. Lower and upper bounds on s_q for square footing and their weighted averages

ϕ	D/B	q_{bL} (LB)	q_{bL} (UB)	$q_{bL,w}$	$d_q\gamma DN_q$	s_q (LB)	s_q (UB)	$s_{q,w}$
25°	0·0	5·10	9·05	5·87	0·00			
	0·1	10·53	14·88	11·37	4·16	1·30	1·40	1·32
	0·2	15·50	21·06	16·58	7·45	1·40	1·61	1·44
	0·4	25·88	34·54	27·56	13·56	1·53	1·88	1·60
	0·6	37·03	49·21	39·39	19·50	1·64	2·06	1·72
	0·8	48·94	65·37	52·13	25·53	1·72	2·21	1·81
	1·0	61·71	82·94	65·83	31·71	1·79	2·33	1·89
	2·0	138·40	198·80	150·12	64·60	2·06	2·94	2·23
30°	0·0	12·67	21·82	14·49	0·00			
	0·1	23·58	34·50	25·75	7·31	1·49	1·74	1·54
	0·2	33·44	47·44	36·22	13·01	1·60	1·97	1·67
	0·4	54·04	76·94	58·59	23·57	1·76	2·34	1·87
	0·6	76·22	109·35	82·80	33·93	1·87	2·58	2·01
	0·8	100·10	145·60	109·14	44·38	1·97	2·79	2·13
	1·0	125·60	185·41	137·49	54·95	2·06	2·98	2·24
	2·0	280·60	429·60	310·21	111·65	2·40	3·65	2·65
35°	0·0	32·96	58·60	38·61	0·00			
	0·1	55·87	85·73	62·45	13·15	1·74	2·06	1·81
	0·2	76·58	117·27	85·55	23·57	1·85	2·49	1·99
	0·4	119·60	188·92	134·88	42·98	2·02	3·03	2·24
	0·6	165·70	265·33	187·66	61·82	2·15	3·34	2·41
	0·8	215·20	347·35	244·33	80·50	2·26	3·59	2·56
	1·0	268·60	432·52	304·73	99·47	2·37	3·76	2·68
	2·0	594·20	959·73	674·77	201·67	2·78	4·47	3·15
40°	0·0	91·04	184·73	112·84	0·00			
	0·1	143·30	260·76	170·64	25·86	2·02	2·94	2·23
	0·2	190·50	341·83	225·72	46·75	2·13	3·36	2·41
	0·4	287·00	508·50	338·55	84·74	2·31	3·82	2·66
	0·6	391·10	683·55	459·16	121·41	2·47	4·11	2·85
	0·8	502·80	876·80	589·84	158·20	2·60	4·37	3·02
	1·0	622·10	1086·60	730·20	195·34	2·72	4·62	3·16
	2·0	1340·00	2385·20	1583·24	390·71	3·20	5·63	3·76
45°	0·0	277·00	683·09	364·79	0·00			
	0·1	412·40	890·12	515·67	56·18	2·41	3·68	2·69
	0·2	533·80	1111·70	658·73	101·32	2·53	4·23	2·90
	0·4	777·50	1599·56	955·21	184·35	2·71	4·97	3·20
	0·6	1029·00	2121·28	1265·13	264·21	2·85	5·44	3·41
	0·8	1307·00	2667·60	1601·13	343·16	3·00	5·78	3·60
	1·0	1601·00	3234·50	1954·13	421·42	3·14	6·05	3·77
	2·0	3344·00	6577·20	4042·95	821·58	3·73	7·17	4·48

a linear relationship between s_γ and B/L for values of B/L less than approximately 0·3, but a more complex trend for $B/L > 0·3$. Their s_γ values were also less than 1 for $\phi < 30°$ and greater than 1 for $\phi > 30°$.

The following equation approximates quite well the shape factor for surface footings calculated using the present analysis:

$$s_\gamma = 1 + (0·0336\phi - 1)\frac{B}{L} \qquad (16)$$

In deriving equation (16), we used the bearing capacity of the square footing for $B/L = 1$. The bearing capacity of the circular footing is slightly greater: the shape factor for a circular footing can be obtained by multiplying that of the square footing under the same conditions by $1 + 0.002\phi$.

There are a number of physical processes whose interaction produces the bearing capacities of strip and finite-size footings. Two competing effects are the larger slip surface area for finite-size footings and the larger constraint/confinement imposed on the mechanism in the case of strip footings. The larger slip surface area (or larger plastic area) that would lead to $s_\gamma > 1$ was observed for circular footings by Bolton & Lau (1993) and by Zhu & Michalowski (2005) using finite element analysis; it was earlier hypothesised by

Meyerhof (1963). In contrast, Vesic (1973) and Brinch Hansen (1970) proposed expressions yielding $s_\gamma < 1$ (refer to Table 1).

Based on our results, it would appear that, for sufficiently low ϕ values, the greater constraint imposed on slip mechanisms in the case of the upper bound or greater confinement imposed on the stress field in the case of the lower-bound method more than compensates for the smaller slip surface area, resulting in $s_\gamma < 1$. But for ϕ values greater than about 30°, which is the range we tend to see in practice, the larger slip surface area dominates, and $s_\gamma > 1$. This contrasts with the Vesic (1973) and Brinch Hansen (1970) equations, popular in practice, which give $s_\gamma < 1$ under all conditions. The physical reasoning that has been advanced in support of these equations is that square and rectangular footings generate smaller mean stress values below the footing, which in turn lead to lower shear strength than that available for a strip footing under conditions of plane strain. However, that argument applies only for footings placed on the surface of identical sand deposits, with the same relative density, for which q_{bL} will indeed be larger for a plane-strain footing (for which ϕ will be higher) than for a circular or rectangular footing with the same width B. If equations in terms of ϕ are used in calculations, that
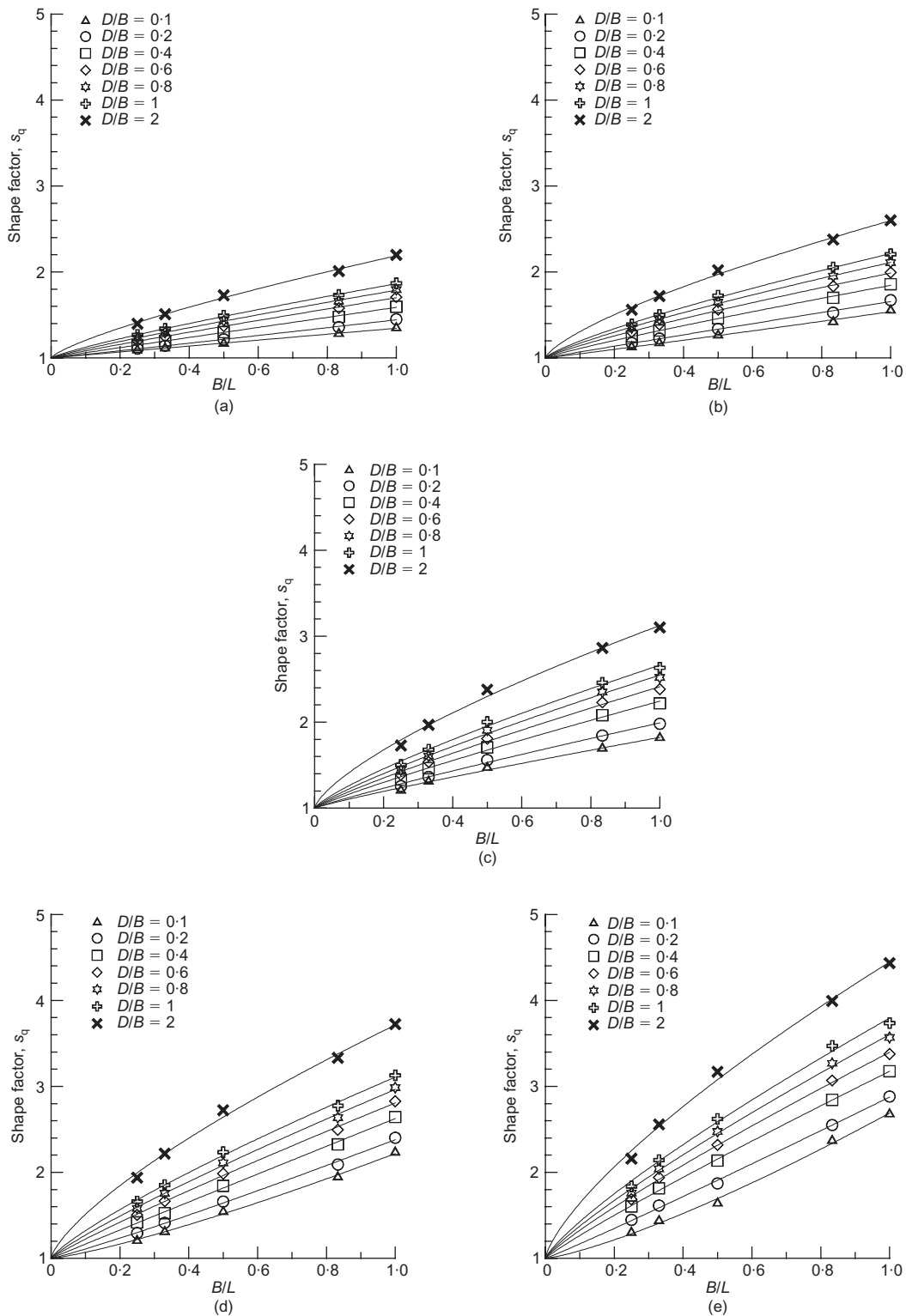
Fig. 14. Shape factor s_q against B/L for various D/B ranging from 0·1 to 2 and: (a) $\phi = 25°$; (b) $\phi = 30°$; (c) $\phi = 35°$; (d) $\phi = 40°$; (e) $\phi = 45°$

difference should not be accounted for by making $s_\gamma < 1$, but rather by taking due account of the lower ϕ for footings in conditions other than plane-strain conditions. So a physical reasoning that does not comprehensively account for all the active processes may lead to the wrong conclusion, as in the case that has been made for s_γ less than 1 for equations written in terms of ϕ.

Determination of s_q

The final factor to determine is the shape factor s_q. Now equation (1) is used directly. We can rewrite it so that s_q is expressed as

$$s_q = \frac{q_{bL} - 0\cdot5(s_\gamma d_\gamma)\gamma B N_\gamma}{d_q q_0 N_q} \tag{17}$$
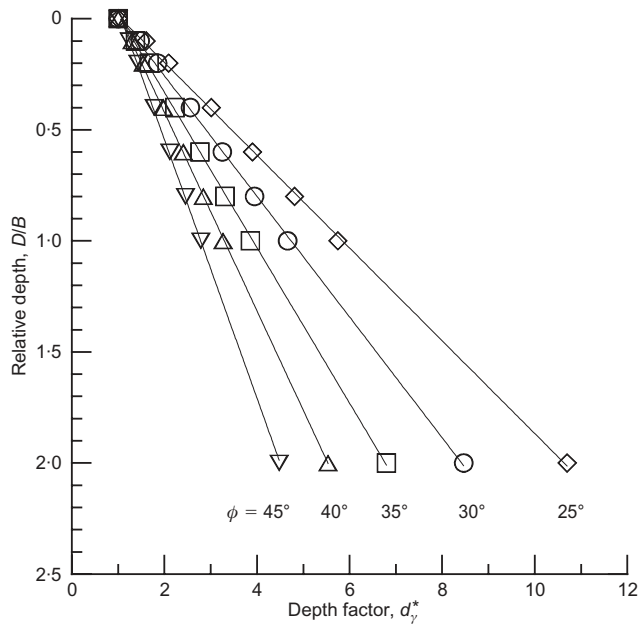
Fig. 15. Depth factor d_γ^*

It is clear that we must know s_γ in order to calculate s_q. Here we make the operational assumption that s_γ is independent of depth. When we make this assumption, we implicitly decide that all of the depth-related effects that were not reflected in the values of d_q, because they are coupled with the footing shape, will be captured by s_q. Calculations are summarised for square footings in Table 7. The results are shown graphically for all values of L/B in Fig. 14. Note that s_q is not defined at $D = 0$, when $q_0 = 0$, and that it must equal 1 for $B/L = 0$ (plane strain). The mathematical form

$$s_q = 1 + f_{q1}\left(\phi, \frac{D}{B}\right)\left(\frac{B}{L}\right)^{f_{q2}\left(\phi, \frac{D}{B}\right)} \tag{18}$$

can be used to fit the results, where functions f_{q1} and f_{q2} of ϕ and D/B must be found such that the fit is optimal. For low ϕ values and $B/L \leqslant 0.5$, the behaviour is very nearly linear, with f_{q2} being approximately equal to 1. The following expression fits the limit analysis results:

$$s_q = 1 + (0.098\phi - 1.64)\left(\frac{D}{B}\right)^{0.7-0.01\phi}\left(\frac{B}{L}\right)^{1-0.16\left(\frac{D}{B}\right)} \tag{19}$$

For small D/B values, equation (19) is approximately linear in B/L. The equation, for $B/L = 1$, may be applied to square footings. For circular footings, the s_q of equation (19) must be multiplied by an additional factor equal to $1 + 0.0025\phi$.

Table 8. Shape and depth factors, s_γ^* and d_γ^*, for circular, square and rectangular footings

ϕ	D/B	q_{bL} (2D)	d_γ^*	Circular		Square		$L/B = 2$		$L/B = 3$	
				q_{bL}	s_γ^*	q_{bL}	s_γ^*	q_{bL}	s_γ^*	q_{bL}	s_γ^*
25°	0·0	6·49	1·00	6·22	0·96	5·87	0·90	6·15	0·95	6·28	0·97
	0·1	10·65	1·64	12·14	1·14	11·37	1·07	10·88	1·02	10·80	1·01
	0·2	13·94	2·15	17·61	1·26	16·58	1·19	15·10	1·08	14·69	1·05
	0·4	20·05	3·09	29·09	1·45	27·56	1·37	23·78	1·19	22·54	1·12
	0·6	25·99	4·01	41·61	1·60	39·39	1·52	33·02	1·27	30·80	1·18
	0·8	32·02	4·93	55·09	1·72	52·13	1·63	43·03	1·34	39·66	1·24
	1·0	38·20	5·89	69·81	1·83	65·83	1·72	54·00	1·41	49·23	1·29
30°	0·0	14·75	1·00	15·65	1·06	14·49	0·98	14·94	1·01	14·98	1·02
	0·1	22·06	1·50	27·76	1·26	25·75	1·17	24·03	1·09	23·40	1·06
	0·2	27·76	1·88	38·99	1·40	36·22	1·30	32·24	1·16	30·83	1·11
	0·4	38·32	2·60	62·63	1·63	58·59	1·53	49·57	1·29	46·22	1·21
	0·6	48·68	3·30	88·45	1·82	82·80	1·70	68·40	1·40	62·52	1·28
	0·8	59·13	4·01	116·66	1·97	109·14	1·85	88·83	1·50	79·89	1·35
	1·0	69·70	4·73	147·25	2·11	137·49	1·97	111·04	1·59	98·59	1·41
35°	0·0	34·48	1·00	41·33	1·20	38·61	1·12	37·84	1·10	36·84	1·07
	0·1	47·63	1·38	68·01	1·43	62·45	1·31	56·97	1·20	54·09	1·14
	0·2	58·05	1·68	92·41	1·59	85·55	1·47	74·63	1·29	69·17	1·19
	0·4	77·46	2·25	143·84	1·86	134·88	1·74	111·71	1·44	100·43	1·30
	0·6	96·30	2·79	199·69	2·07	187·66	1·95	150·83	1·57	132·99	1·38
	0·8	114·98	3·33	258·67	2·25	244·33	2·12	193·34	1·68	168·06	1·46
	1·0	133·95	3·88	323·47	2·41	304·73	2·28	239·99	1·79	206·57	1·54
40°	0·0	85·57	1·00	121·45	1·42	112·84	1·32	100·19	1·17	94·41	1·10
	0·1	111·43	1·30	184·61	1·66	170·64	1·53	141·46	1·27	129·80	1·16
	0·2	132·32	1·55	242·56	1·83	225·72	1·71	179·56	1·36	162·30	1·23
	0·4	170·31	1·99	361·46	2·12	338·55	1·99	258·87	1·52	226·05	1·33
	0·6	206·98	2·42	490·93	2·37	459·16	2·22	344·64	1·67	299·72	1·45
	0·8	243·77	2·85	628·18	2·58	589·84	2·42	438·67	1·80	376·67	1·55
	1·0	280·91	3·28	779·86	2·78	730·20	2·60	542·80	1·93	461·57	1·64
45°	0·0	234·21	1·00	398·80	1·70	364·79	1·56	296·19	1·26	275·26	1·18
	0·1	290·39	1·24	568·77	1·96	515·67	1·78	399·94	1·38	364·86	1·26
	0·2	335·53	1·43	724·32	2·16	658·73	1·96	498·41	1·49	448·61	1·34
	0·4	418·56	1·79	1040·75	2·49	955·21	2·28	704·88	1·68	621·22	1·48
	0·6	498·42	2·13	1379·80	2·77	1265·13	2·54	925·73	1·86	800·91	1·61
	0·8	577·37	2·47	1729·87	3·00	1601·13	2·77	1164·91	2·02	991·13	1·72
	1·0	655·63	2·80	2120·67	3·23	1954·13	2·98	1422·37	2·17	1195·08	1·82

Alternative form of bearing capacity equation for sands

As noted both in the present paper and in Salgado *et al.* (2004) for clays, shape and depth factors are interdependent, in contrast with the assumption that it is necessary to propose a bearing capacity equation of the form of equation (1). Whereas in the preceding subsections we retained the traditional form of the bearing capacity equation, and determined expressions for s_q, s_γ, d_q and d_γ that take due account of the interdependence of all quantities, we shall now explore an alternative form of the bearing equation that is simpler and does not attempt to dismember bearing capacity into artificial components.

A much simplified form of the bearing capacity equation can be proposed now that numerical limit analysis allows the overburden to be treated as a soil and not a surcharge. When we do that, the N_q term completely disappears, and we are left with

$$q_{bL} = \frac{1}{2}\gamma B s_\gamma^* d_\gamma^* N_\gamma \qquad (20)$$

As before, we follow tradition and separate depth and shape effects in equation (20) by using two factors (d_γ^* and s_γ^*). If we set d_γ^* as a function of depth only, we can use equation (20) to calculate the bearing capacity of strip footings, for which s_γ^* is 1. For rectangular and circular footings, we find that s_γ^* depends not only on B/L but also on depth.

Using the same data as before, we can calculate d_γ^* by using

$$d_\gamma^* = \frac{q_{bL,strip}\big|_{\frac{D}{B}}}{q_{bL,strip}\big|_{\frac{D}{B}=0}} \qquad (21)$$

Figure 15 shows the depth factor, calculated as per equation (21), against D/B for the five values of friction angle considered. The relationship between d_γ^* and D/B is almost perfectly linear. The following equation represents the straight lines shown in the figure quite well:

$$d_\gamma^* = 1 + (8 \cdot 404 - 0 \cdot 151\phi)\frac{D}{B} \qquad (22)$$

where the friction angle is given in degrees.

The shape factor is calculated for a given D/B value as

$$s_\gamma^* = \frac{q_{bL}\big|_{\frac{B}{L}}}{q_{bL,strip}} \qquad (23)$$

The value of s_γ^* for $D/B = 0$ is obviously the same as s_γ, given by equation (16). The ratio of s_γ^* to s_γ is therefore a function of D/B and B/L that takes the value of 1 at $D/B = 0$. The following equation captures this relationship quite well:

$$\frac{s_\gamma^*}{s_\gamma} = 1 + \left(0 \cdot 31 + 0 \cdot 95\frac{B}{L}\right)(2 \cdot 63 + 0 \cdot 023\phi)\left(\frac{D}{B}\right)^{1 \cdot 15 - 0 \cdot 54\frac{B}{L}} \qquad (24)$$

In deriving the depth and shape factors, we assumed d_γ^* to be independent of shape, with the result that the shape factor depends on depth, as clearly shown by equation (24). When we multiply together the shape factor and depth factor in equation (20), the issue of whether it is the depth factor that depends on B/L or the shape factor that depends on D/B disappears. In other words, the same final equation would have resulted had we assumed the shape factor to be independent of depth and the depth factor to depend on B/L, or, put more simply, had we assumed a single correction factor, function of ϕ, B/L and D/B.

All computed values of d_γ^* and s_γ^* for considered footing shapes and the ranges of D/B and ϕ are prsented in Table 8.

SUMMARY AND CONCLUSIONS

Rigorous upper- and lower-bound analyses of circular, rectangular and strip footings in sand have been performed. The analyses provided ranges within which the exact collapse loads for the footings are to be found. This study became possible because of the development of efficient algorithms for optimisation of stress fields for lower-bound analysis and velocity fields for upper-bound analysis.

We have also examined the traditional bearing capacity equation and the underlying assumptions of superposition of surcharge and self-weight terms and independence of shape factors from depth and depth factors from shape of the footings. It was found that these assumptions are not valid. We proposed new shape and depth factors that do account for the interdependence of all the terms. Additionally, the derivation of these factors did not require making the assumption of superposition.

An alternative bearing capacity equation with a single term is simpler than the traditional form of the bearing capacity equation. For surface strip footings, the equation reduces to the traditional $\frac{1}{2}\gamma B N_\gamma$ form. Depth is accounted for by multiplying this term by a depth factor d_γ^*, and shape by multiplication by a shape factor s_γ^*. As shape and depth are not truly independent, the final equation can be viewed as simply the basic $\frac{1}{2}\gamma B N_\gamma$ term multiplied by factors that are functions of B/L and D/B.

REFERENCES

Bolton, M. D. (1979). *A guide to soil mechanics*. London: Macmillan; reprinted by Chung Hwa Books, and published by M. D. and K. Bolton in 1998.

Bolton, M. D. & Lau, C. K. (1993). Vertical bearing capacity factors for circular and strip footings on Mohr−Coulomb soil. *Can. Geotech. J.* **30**, No. 6, 1024−1033.

Booker, J. R. (1969). *Applications of theories of plasticity to cohesive frictional soils*. PhD thesis, Sydney University.

Brinch Hansen, J. (1963). Cited once with different year in text.

Brinch Hansen, J. (1970). *A revised and extended formula for bearing capacity*, Bulletin No. 28. Lyngby: Danish Geotechnical Institute.

Caquot, A. & Kerisel, J. (1953). Sur le terme de surface dans le calcul des fondations en milieu pulverent. *Proc. 3rd Int. Conf. Soil Mech. Found. Engng, Zurich* **1**, 336−337.

Davis, E. H. & Booker, J. R. (1971). The bearing capacity of strip footings from the standpoint of plasticity theory. *Proc. 1st Australian-New Zealand Conf. on Geomechanics, Melbourne*, 275−282.

De Beer, E. E. (1970). Experimental determination of the shape factors and the bearing capacity factors of sand. *Géotechnique* **20**, No. 4, 387−411.

Drucker, D. C., Greenberg, W. & Prager, W. (1951). The safety factor of an elastic-plastic body in plane strain. *Trans. ASME, J. Appl. Mech.* **73**, 371−378.

Drucker, D. C., Prager, W. & Greenberg, H. J. (1952). Extended limit design theorems for continuous media. *Q. Appl. Math.* **9**, No. 4, 381−389.

Erickson, H. L. & Drescher, A. (2002). Bearing capacity of circular footings. *J. Geotech. Geoenviron. Engng ASCE* **128**, No. 1, 38−43.

Hansen, B. & Christiansen, N. H. (1969). Discussion of 'Theoretical bearing capacity of very shallow footings' by A. L. Larkin. *J. Soil Mech. Found. Div. ASCE* **95**, No. SM6, 1568−1567.

Hill, R. (1951). On the state of stress in a plastic-rigid body at the yield point. *Phil. Mag.* **42**, 868−875.

Krabbenhøft, K., Lyamin, A. V., Hijaj, M. & Sloan, S W. (2005). A new discontinuous upper bound limit analysis formulation. *Int. J. Numer. Methods Engng.* **63**, No. 7, 1069−1088.

Lyamin, A. V. (1999). *Three-dimensional lower bound limit analysis*

using nonlinear programming. PhD thesis, Department of Civil, Surveying and Environmental Engineering, University of Newcastle, NSW, Australia.

Lyamin, A. V. & Sloan, S. W. (2002a). Lower bound limit analysis using nonlinear programming. *Int. J. Numer. Methods Engng* **55**, No. 5, 573–611.

Lyamin, A. V. & Sloan, S. W. (2002b). Upper bound limit analysis using linear finite elements and nonlinear programming. *Int. J. Numer. Anal. Methods Geomech.* **26**, No. 2, 181–216.

Lyamin, A. V., Krabbenhøft, K., Abbo, A. J. & Sloan, S. W. (2005). General approach to modelling discontinuities in limit analysis. *Proc. 11th Int. Conf. Int. Assoc. Computer Methods and Advances in Geomechanics (IACMAG 2005), Torino* **1**, 95–102.

Makrodimopoulos, A. & Martin, C. M. (2005). *Upper bound limit analysis using simplex strain elements and second-order cone programming*, Technical Report 2288/2005. University of Oxford.

Martin, C. M. (2005). Exact bearing capacity calculations using the method of characteristics. *Proc. 11th Int. Conf. IACMAG, Turin* **4**, 441–450.

Meyerhof, G. G. (1951). The ultimate bearing capacity of foundations. *Géotechnique* **2**, No. 4, 301–332.

Meyerhof, G. G. (1963). Some recent research on bearing capacity of foundations. Can. Geotech. J. **1**, No. 1, 16–26.

Pastor, J. (1978). Analyse limite: determination de solutions statiques completes. Application au talus vertical. *Eur. J. Mech. A/Solids* **2**, No. 2, 176–196.

Reissner, H. (1924). Zum Erddruckproblem. *Proc. 1st Int. Cong. Applied Mechanics, Delft*, 295–311.

Salgado, R. (2008). *The engineering of foundations*. McGraw-Hill.

Salgado, R., Lyamin, A., Sloan, S. & Yu, H. S. (2004). Two- and three-dimensional bearing capacity of footings in clay. *Géotechnique* **54**, No. 5, 297–306.

Smith, C. C. (2005). Complete limiting stress solutions for the bearing capacity of strip footings on a Mohr–Coulomb soil. *Géotechnique* **55**, No. 8, 607–612.

Terzaghi, K. (1943). *Theoretical soil mechanics*. New York: Wiley.

Vesic, A. S. (1973). Analysis of ultimate loads of shallow foundations. *J. Soil Mech. Div. ASCE* **99**, No. SM1, 45–73.

Yu, H. S., Sloan, S. W., and Kleeman, P. W. (1994). A quadratic element for upper bound limit analysis. *Engng Comput.* **11**, No. 3, 195–212.

Zhu, M. & Michalowski, R. L. (2005). Shape factors for limit loads on square and rectangular footings. *J. Geotech. Geoenviron. Engng* **131**, No. 2, 223–231.